

Alma Mater Studiorum Università di Bologna
Archivio istituzionale della ricerca

C60@lysozyme: A new photosensitizing agent for photodynamic therapy

This is the final peer-reviewed author's accepted manuscript (postprint) of the following publication:

Published Version:

Soldă , A., Cantelli, A., Di Giosia, M., Montalti, M., Zerbetto, F., Rapino, S., et al. (2017). C60@lysozyme: A new photosensitizing agent for photodynamic therapy. JOURNAL OF MATERIALS CHEMISTRY. B, 5(32), 6608-6615 [10.1039/c7tb00800g].

Availability:

This version is available at: <https://hdl.handle.net/11585/616887.4> since: 2018-11-13

Published:

DOI: <http://doi.org/10.1039/c7tb00800g>

Terms of use:

Some rights reserved. The terms and conditions for the reuse of this version of the manuscript are specified in the publishing policy. For all terms of use and more information see the publisher's website.

This item was downloaded from IRIS Università di Bologna (<https://cris.unibo.it/>).
When citing, please refer to the published version.

(Article begins on next page)

Accepted manuscript of

C₆₀@lysozyme: a new photosensitizing agent for photodynamic therapy

Soldà , A.; Cantelli, A.; Di Giosia, M.; Montalti, M.; Zerbetto, F.; Rapino, S.; Calvaresi, M.

Dipartimento di Chimica “G. Ciamician”, Alma Mater Studiorum – Università di Bologna, via F. Selmi 2, 40126 Bologna, Italy.

Corresponding author: E-mail: matteo.calvaresi3@unibo.it.

N.B.: When citing this work, cite the original article

Original Publication:

Soldà , A.; Cantelli, A.; Di Giosia, M.; Montalti, M.; Zerbetto, F.; Rapino, S.; Calvaresi, M.

C₆₀@lysozyme: a new photosensitizing agent for photodynamic therapy. *J. Mater. Chem. B*, 2017, **5, 6608-6615.**

DOI: [10.1039/c7tb00800g](https://doi.org/10.1039/c7tb00800g)

Copyright: Royal Society of Chemistry. <http://www.rsc.org/>

Postprint available at:

<https://cris.unibo.it/handle/11585/616887#.W-rdkTFRfcs>

(PDF) C₆₀@lysozyme: a new photosensitizing agent for photodynamic therapy. Available from:

<https://pubs.rsc.org/en/Content/ArticleLanding/2017/TB/C7TB00800G#!divAbstract>

[accessed Nov 13 2018]



C₆₀@lysozyme: a new photosensitizing agent for photodynamic therapy

Received 00th January 20xx,
Accepted 00th January 20xx

DOI: 10.1039/x0xx00000x

www.rsc.org/

A. Soldà,[†] A. Cantelli,[†] M. Di Giosia, M. Montalti, F. Zerbetto, S. Rapino and M. Calvaresi*

C₆₀@lysozyme showed significant visible light-induced singlet oxygen generation in water, indicating the potential of this hybrid as an agent for photodynamic therapy. The reactive oxygen specie (ROS) concentration generated by C₆₀@lysozyme during the irradiation depends on the light source, the irradiation time and the concentration of the hybrid. C₆₀@lysozyme significantly reduced HeLa cells viability in response to visible light irradiation. The generation of H₂O₂, due to the photoactivity of C₆₀@lysozyme, causes cell death via hydrogen peroxide easy permeation through the cell membrane and activation of endogenous ROS production.

Introduction

Photodynamic therapy (PDT) is a non-invasive treatment for different types of cancer.¹ The combination of a photosensitizing agent and focused irradiation is used to elicit local, controlled production of reactive oxygen species (ROS) in a specific area, leading to cell death through several pathways.¹ In fact, ROS react with a wide range of biological targets and are known to be involved in both cellular signaling and cell damage.¹ By using highly focused light irradiation, PDT has the potential to act specifically at the desired site of action, lowering collateral damage to healthy cells.¹

Photosensitization is a simple and controllable method for the production of ¹O₂, requiring only oxygen, light of the appropriate wavelength, and a photosensitizing agent able of absorbing and using the energy to excite oxygen to its singlet state.

Fullerenes are extremely efficient singlet oxygen generators with the quantum yield of ¹O₂ that is close to the unity, suggesting the use of fullerenes in PDT.

Fullerenes strongly absorb in the UV and moderately in the visible regions of the spectrum. The singlet excited state of C₆₀ (¹C₆₀*), initially formed upon light absorption, is followed by conversion to the long lived triplet state (³C₆₀*) through an intersystem crossing with high quantum yield (nearly 100%) that can be efficiently quenched by molecular oxygen (³O₂) to generate large amounts of singlet oxygen (¹O₂) (type II energy-transfer pathway).²⁻⁵

However, the excited triplet state of fullerene is also an

excellent electron acceptor, and, in the presence of electron donors, gives the C₆₀ radical anion (C₆₀^{•-}) via a type I electron-transfer pathway that can readily transfer the electron to molecular oxygen forming the superoxide anion radical (O₂^{•-}) and other reactive species.²⁻⁵

In the last decade, fullerenes have gained considerable attention as potentials photosensitizer for PDT of various diseases.⁵⁻⁶⁴

Fullerenes possess considerable advantages over the traditional photosensitizer used in photodynamic therapy:

- Fullerenes are highly photostable and undergo less photobleaching compared to the traditional dyes used in PDT;²⁻¹¹
- Fullerenes follow both the photophysical mechanisms, while the traditional dyes show mainly type II mechanism;²⁻¹¹
- The reactive oxygen species production yield is close to unity;²⁻¹¹

However, the use of fullerenes in PDT still presents important restrictions in their application due to the dependency of their properties and toxicity on the physiological environment and the related aggregation phenomena⁶⁵ and their poor water solubility and low biocompatibility.⁶⁵

Monodispersity of fullerenes is the crucial feature for potential application in PDT:^{12,14,65} Aggregation is a well-known factor that could deactivate the excited electronic states of photosensitizers.²⁻¹¹ In fact, aggregation drastically decreases the long-lived triplet excited state lifetime, consequently reducing the ROS production efficiency. ³C₆₀*, the indispensable intermediate to produce ROS, is highly sensitive to the environment. When fullerenes aggregates are present, ³C₆₀* can be easily quenched by the surrounding C₆₀ or by other ³C₆₀* (triplet-triplet annihilation) and, consequently, the lifetime is drastically reduced (from a hundreds of μs for monomeric C₆₀ to less than 0.1 μs in a C₆₀ aggregate).²⁻¹¹

In addition aggregation reduces also the active surface area of C₆₀ in contact with O₂ for ROS production.

Dipartimento di Chimica "G. Ciamician", Alma Mater Studiorum - Università di Bologna, via F. Selmi 2, 40126 Bologna, Italy
E-mail: matteo.calvaresi3@unibo.it

[†] These authors contributed equally to this work

Electronic Supplementary Information (ESI) available: [details of any supplementary information available should be included here]. See DOI: 10.1039/x0xx00000x

Fullerenes are insoluble in water and in most polar media. Different approaches have been used to overcome the lack of solubility of fullerene:

1) Dispersion of nano- C_{60} aggregates in water by mechanical dispersion–stabilization of C_{60} ,⁶⁶ either through ultrasonication⁶⁷ or by solvent-exchange methods.⁶⁸ Although these preparation methods increase pristine C_{60} concentration in aqueous solution, they generate metastable dispersions of fullerenes containing large aggregates. These nano- C_{60} nanoparticles eventually re-aggregate, especially in physiologically environments, because the method does not provide a way to overcome the strong fullerene-fullerene interactions. Considering the PDT application of fullerenes, ROS producing ability of fullerene decreases with the growing size of aggregation, so this methodology is not effective for real medical exploitation.

2) Synthesis of water-soluble fullerene derivatives by chemical functionalization, with hydrophilic groups, of pristine fullerene.^{69,70} This method, even if very effective for many technological applications of fullerenes, shows some limitations for PDT, because functionalization of C_{60} cage leads to the alterations of the peculiar photophysical properties of fullerenes, thus reducing the advantages of the use of fullerene in PDT. In fact, the properties of functionalized fullerenes strongly dependent on the number of functional groups linked to the cage, for example the triplet quantum yield significantly decreases as the number of pendant increase.³ In addition in polar solvents, as physiological environment, the hydrophobic nature of fullerene leads them to cluster together, leaving the hydrophilic functional groups outside.

3) A very common approach, especially for PDT applications, is the use of dispersants as surfactants, block copolymers, amphiphilic polymers, micelles and liposomes.^{51–61} The use of dispersants is effective and a large quantity of C_{60} can be dispersed also in water, but i) the resulting solutions are characterized by a polydispersion of fullerene aggregates of different sizes and ii) the fullerenes are screened inside the micelles, reducing the contact with active O_2 molecules.

4) Dispersion of fullerenes via host-guest interactions with suitable carriers endowed with hydrophobic cores, such as cyclodextrins, calixarenes, and other nanotweezers or macrocyclic receptors.⁷² The supramolecular approach generates monodispersed pristine fullerenes, but subsequent aggregation of the inclusion complexes⁷³ is common, especially in saline solutions as physiological environment. In addition the use of these hosts for biological applications sometimes may be problematic because of their intrinsic toxicity.⁷⁴

A pioneering approach to the use of proteins as biocompatible hosts for fullerene derivative in PDT was proposed by Tsuchida and coworkers.⁶³ The use of proteins as molecular host for a PDT agent eliminate also problems due to aggregation and potential toxicity of macrocyclic receptors. We used lysozyme as a model protein because it is one of the less expensive, more deeply understood, and most used proteins in research. In addition we recently showed that lysozyme is able to disperse monomolecularly in water even the pristine C_{60} with a

1:1 stoichiometry. NMR and photophysical studies demonstrated that lysozyme maintains its tridimensional structure upon interaction with C_{60} and that the fullerene binds selectively in the protein substrate binding pocket.^{75,76} Proteins are able to interact with the hydrophobic cage of fullerene via π - π stacking interactions, hydrophobic interactions, surfactant-like interactions, and charge- π interactions.^{75–80}

In this paper we show that the C_{60} @lysozyme hybrid can be potentially exploited in PDT therapy.

Materials and Methods

Materials.

Lysozyme from chicken egg white lyophilized powder (Cat. N° L6876), fullerene- C_{60} (Cat. n° 483036) and Type VI-A Peroxidase from horseradish lyophilized powder (Cat. n° P6782) were purchased from Sigma Aldrich. For the photoirradiation experiments the compounds were dissolved in Dulbecco's Phosphate Buffered Saline 10X (Cat. n° X0515) diluted in Milli-Q water. For centrifuge filtration, 3K Amicon Ultra-0.5 Centrifugal Filter Units with Ultracel-3 membrane (Cat. n° UFC500324) was used. Dulbecco's Modified Eagle's Medium (DMEM), DMEM without glucose, sodium pyruvate and red phenol, fetal bovine serum (FBS) South-America, L-glutamine and penicillin-streptomycin were purchased from Gibco-Life Technologies Corporation. β -D-glucose BioXtra \geq 99.5%, sodium pyruvate, 2'-7'-dichlorofluorescein diacetate (DCFH-DA Cat. n° 35848) were purchased from Sigma Aldrich. Hydrogen peroxide (H_2O_2 33% w/v) was purchased from Panreac, PBS (pH 7.4) from Lonza and Milli-Q water from Millipore.

Light Sources

Low-power energy source. A 6W warm white (3000 K) Light-Emitting Diode (LED) bulb purchased from BTEK® was used as a low-power light source. The bulb dimension is \varnothing 50 x 61 mm with a beam angle of 120°. The LED irradiance is around 0.064 mWcm⁻² in 400–750 nm wavelength range. To have a homogeneous area of irradiation, the samples were placed under the LED source at distance of 25 cm during treatment.

High-power energy source. A SANOLUX HRC 300-280 E27 lamp operating in the 400–750 nm wavelength range purchased from Osram was used. To have a homogeneous area of irradiation the samples were placed under the light sources at the distance of 50 cm from the lamp providing an irradiance of 1.6 mWcm⁻² on the samples during treatment.

Synthesis of C_{60} @Lysozyme

The adduct C_{60} @lysozyme was synthesized as described previously.⁷⁵ C_{60} powder was used in 2:1 excess with respect to the stoichiometric relationship, to 1 mL of a 1 mM solution of lysozyme in Milli-Q water. After sonication for 60 min using a probe tip sonicator (Hielscher - Ultrasonic Processor UP200St, equipped with the sonotrode S26d7, used at 45% of the maximum amplitude) in an ice bath, C_{60} was dispersed in the lysozyme solution forming a dark brown mixture. A dark-

brown solution was obtained after centrifugation at 10600 g for 10 min and the collection of the supernatant. In order to eliminate possible ROS generated during the sonication process, the solution has been washed four times with the 3K Amicon Ultra-0.5 Centrifugal Filter Units, using a volume of 500 μ L and spinning at 14000 g for 20 minutes, obtaining a concentration factor of 8. After each spin the volume of the concentrated solution has been brought back to its original value using Milli-Q water.

Detection of singlet oxygen generation. Singlet oxygen emission spectra were recorded with a spectrofluorimeter Edinburgh FLS920 equipped with a Ge detector for emission in the NIR spectral region. Correction of the emission spectra for detector sensitivity in the 1200–1400 nm spectral region was performed.

ROS production of C₆₀@Lysozyme in PBS buffer

C₆₀@lysozyme irradiation. C₆₀@lysozyme solutions in PBS 10 mM pH 7.4 have been irradiated in the visible range in PMMA cuvettes (optical path 1 cm), both with a high power and a low power light source. During the irradiation process the cuvettes, containing 2.5 mL of solution, have been kept under vigorous stirring.

ROS quantification. The amount of ROS generated during the process has been assessed immediately after irradiation using the DCFH spectrofluorimetric test.⁸¹

DCFH was prepared from DCFH-DA by mixing 0.5 mL of 1.0 mM DCFH-DA in methanol with 2.0 mL of 0.01M NaOH. The hydrolysis reaction of DCFH-DA proceeded at room temperature for 30 min, and the mixture was then neutralized with 10 mL of 25 mM NaH₂PO₄, pH 7.4. This solution was kept on ice in the dark until use.⁸¹ 25 μ L of a solution of HRP 0.1 mg/mL in PBS 10 mM, pH 7.4, and 125 μ L of the prepared solution of DCFH was added to each cuvette for ROS quantification.⁸²

For all the samples, after an incubation time of 30 minutes, fluorescence measurements (Edinburgh Analytical Instruments FLS920, equipped with a photomultiplier Hamamatsu R928P) have been performed. The fluorescence signal was converted to the concentration of ROS produced during the irradiation using a calibration curve created using hydrogen peroxide standard solutions (Figure S1).

Cell Culture

Human cervical adenocarcinoma (HeLa) cell line was used as *in vitro* model. Cells were cultured in Dulbecco's Modified Eagle's Medium (DMEM) supplemented with 10% fetal bovine serum (FBS) South-America, 2mM L-glutamine and 50 U/mL penicillin-streptomycin, the sterile culturing media was filtered by means of 0.20 μ m filters (Millipore) just before the use. Cells were growth in incubator at 37°C, 5% CO₂, 21% O₂ and were passed upon trypsin digestion every four days avoiding cells to reach full confluence.

In vitro measurement of C₆₀@lysozyme photodynamic activity

To measure the photodynamic activity of C₆₀@lysozyme, HeLa cells were plated at a density of 4×10^3 cells per well in 24-well plates. After overnight incubation, the cells were treated with C₆₀@lysozyme in serum-free and red phenol-free medium. Half of the samples were exposed to the light source, while the others were incubated in absence of any exposure to light (dark condition). Cell viability was conducted after 24 h of incubation upon photo-irradiation.

Cell viability studies. Cell viability was assessed by using erythrosine B exclusion assay. Cell survival was expressed as the percentage ratio of viable treated cells in comparison with the corresponding viable untreated controls. For statistical elaboration and IC₅₀ calculation, OriginPro Software was used. Reported data corresponded to mean value \pm standard deviation (SD) from at least three different experiments.

Measurement of intracellular Reactive Oxygen Species (ROS)

The measurement of intracellular ROS was based on the detection of the fluorescence due to the oxidation of 2,7-dichlorohydrofluorescein diacetate (DCFH-DA). DCFH-DA passively enters the cells and then reacts with ROS to form a highly fluorescent compound dichlorofluorescein (DCF).⁸¹

C₆₀@lysozyme treatment. HeLa cells were plated at a density of 6×10^4 cells per well in 35 mm Petri dishes. After overnight incubation at 37°C, 5% CO₂, the cells were washed with PBS and incubated with 100 μ M DCFH-DA in PBS for 30 min, washed and maintained in complete medium for 30 min to avoid any nonspecific artifacts.⁸³ The cells were then treated with C₆₀@lysozyme in serum-free and red phenol-free medium and irradiated for 10 min with the high-power energy light source. Cells were kept in incubation for other 30 min and then washed three times with PBS before analysis.

H₂O₂ treatment. HeLa cells were plated at a density of 6×10^4 cells per well in 35 mm Petri dishes. After overnight incubation at 37°C, 5% CO₂, the cells were washed with PBS buffer and incubated with 100 μ M of DCFH-DA in PBS for 30 min, washed and maintained in complete medium for 30 min to avoid any nonspecific artifacts.⁸³ Then, the cells were treated with a solution containing 200 μ M of hydrogen peroxide for 30 min, 1h and 3h. The cells were washed three times with PBS before analysis.

The fluorescence of DCF was observed using an inverted Ti-S Nikon microscope equipped with a fluorescence module employing a mercury lamp and using a 494 nm excitation and 518 nm emission filter. The fluorescence signal was captured using a QImaging Retiga-2000RV CCD digital camera. The mean values of the fluorescence intensities were estimated by using the histogram intensity profiles of the images, obtained with the same exposure settings, from at least thirty different cells.

Statistical analysis.

Statistical elaboration of the data was carried out using the OriginPro Software. Statistical significance was established using one-way ANOVA test. *P* values < 0.05 (*), < 0.01 (**), < 0.001 (***) were considered as statistically significant.

Results and Discussion

C_{60} @lysozyme adducts were prepared by the method developed previously⁷⁵ and reported in the Materials and Methods section. C_{60} is highly hydrophobic and insoluble in most polar solvents, especially water. We prepared monodispersed fullerenes by complexation with lysozyme in the form of C_{60} @lysozyme, forming a noncovalent supramolecular complex. The obtained yellow water solution is stable for months and once formed C_{60} @lysozyme adduct does not dissociate.

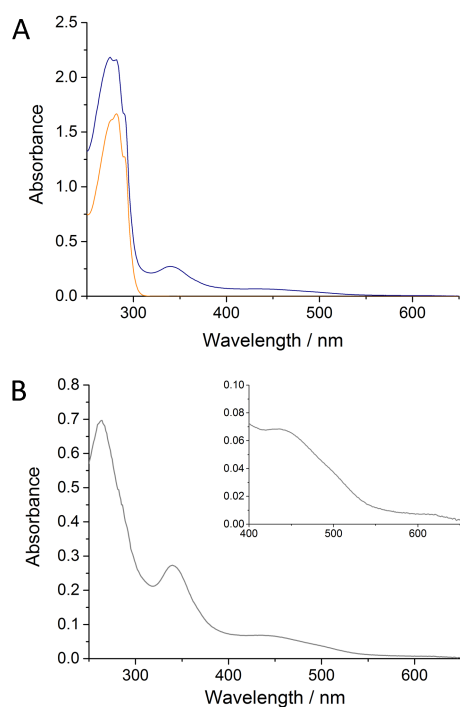


Figure 1. Spectroscopic characterization of C_{60} @lysozyme hybrid. A) UV-visible spectra of lysozyme (orange line) and C_{60} @lysozyme hybrid (blue line). B) Differential spectrum of C_{60} (C_{60} @lysozyme-lysozyme). The inset shows the absorbance of the C_{60} @lysozyme hybrid in the visible range 400-650 nm.

The UV-visible spectrum of C_{60} @lysozyme (Figure 1A) revealed features that belong to both components of the hybrid, showing the distinctive absorption of C_{60} (341 nm) and of the protein (281 nm). In addition to the diagnostic bands of C_{60} at 260 and 341 nm, it is evident an absorption bands in the 400-600 nm range (see also the differential spectrum of C_{60} , Figure 1B, and the inset) that can be potentially exploited for PDT therapy.

Detection of singlet oxygen generation by C_{60} @lysozyme

Preliminary measurements to test the photosensitizing ability of C_{60} @lysozyme hybrid to produce singlet oxygen (1O_2) in water upon visible light irradiation were carried out measuring the near IR emission of 1O_2 around 1270 nm, due to the singlet oxygen phosphorescence which corresponds to the O_2 ($^1\Delta_g$) - O_2 ($^3\Sigma_g^-$) transition. This measurement is considered the most reliable direct observation of 1O_2 system. The 1O_2 emission

spectrum obtained after irradiation of the C_{60} @lysozyme with a Xenon lamp, excitation at 514 nm, is shown in Figure 2, clearly indicating that C_{60} @lysozyme hybrid upon irradiation is able in water to produce singlet oxygen. C_{60} @lysozyme shows a singlet oxygen quantum yield higher than Rose Bengal ($\Phi_D=0.76$) (see Figure S3).

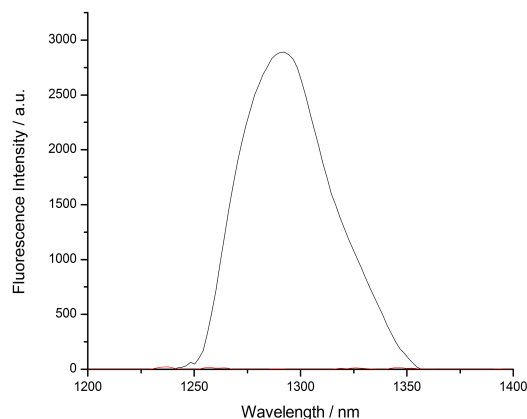


Figure 2. Emission spectra from singlet oxygen generated upon excitation at 514 nm for a solution 1 mM of C_{60} @lysozyme (black line) and lysozyme (red line)

ROS Generation Ability of C_{60} @lysozyme in PBS buffer

To evaluate quantitatively the photosensitizing ability of C_{60} @lysozyme adducts, an optimized DCFH methodology, specifically developed for nanoparticles⁸² was used to measure the generation of ROS upon irradiation by visible light. In the presence of ROS, DCFH is rapidly oxidized to the highly fluorescent 2',7'-dichlorofluorescein (DCF), allowing ROS quantification in solution (Figure 3).

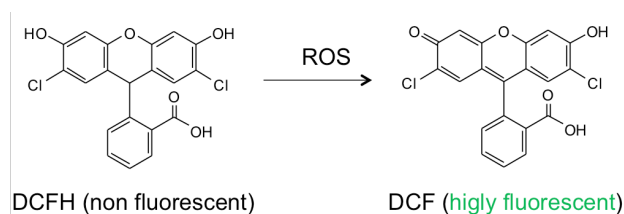


Figure 3. Oxidation of DCFH by ROS to produce the highly fluorescent DCF

Before the experiments, the C_{60} @lysozyme solution was carefully washed using 3K Vivaspin® in order to eliminate possible ROS generated during the sonication process.⁸⁴ The ability to generate ROS by C_{60} @lysozyme in PBS, for different concentrations (Figure 4A) where the adduct is stable and for different irradiation times (Figure 4B) were investigated. The concentration of C_{60} @lysozyme was estimated using the absorbance band at 341 nm. Two irradiation sources, with different intensity, were used. The ROS concentration generated during the irradiation is plotted as difference between the signals of the C_{60} @lysozyme samples and that of the reference, i.e. lysozyme, with the

same protein concentration of the C₆₀@lysozyme samples, and under the same lightning conditions.

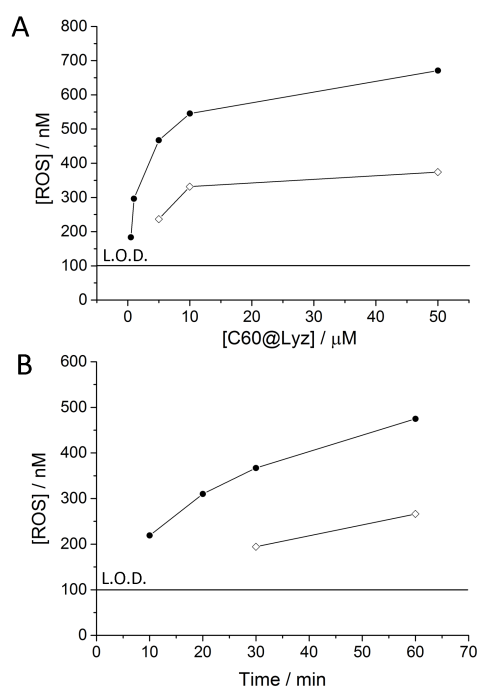


Figure 4. ROS generated by A) different concentrations of C₆₀@lysozyme B) different irradiation times; using a mild light source (white diamonds) or a strong light source (black dots).

The changes in fluorescence intensity of DCF reveal ROS generation from the C₆₀@lysozyme solution. Figure 4 shows ROS generation from C₆₀@lysozyme during visible light illumination. It appears that:

- Strong illumination is able to produce more ROS than mild illumination,
- The generated ROS are proportional to the concentration of C₆₀@lysozyme. This trend, as function of C₆₀@lysozyme concentration, supports the monodispersed state of C₆₀ molecules in solution, since no detrimental variation in the generation of ROS are observed by increasing the C₆₀ concentration as commonly happens when aggregation phenomena occur.^{12,65,85}
- The C₆₀@lysozyme exhibited an increased generation of ROS at increasing irradiation times.

Control experiments with the same C₆₀@lysozyme solutions at different concentrations kept in the dark showed consistently signals below the limit of detection of the assay, confirming that the C₆₀@lysozyme is photoactive only upon visible light irradiation.

Phototoxicity of C₆₀@lysozyme in HeLa cells by Visible Light Irradiation.

To assess *in vitro* the cytotoxicity of C₆₀@lysozyme upon irradiation, the ability of the hybrid to inhibit growth and induce cell death upon photoexcitation with visible light was tested. HeLa cells, a highly proliferative *in vitro* human cancer model, were used. The survival of HeLa cells in the presence or

in the absence of light irradiation was measured by using the erythrosine B exclusion assay. Erythrosine is a membrane-impermeable dye, which is included upon dead cells with a leaky membrane and is kept out by living cells with an intact plasma membrane. No reduction in the untreated cell viability was observed upon the irradiation of the cells with the visible light low-energy power source (Figure S2).

On the contrary, the presence of C₆₀@lysozyme caused a marked reduction in the viability of HeLa cells in a dose dependent manner, when irradiated with the same light source (Figure 5). The results show that the cell survival rate is related to the concentration of the photosensitizer present in the cell medium. As the concentration of C₆₀@lysozyme increases, the cell viability decreases. Upon treatment with 5 μ M of C₆₀@lysozyme the percentage of survival cells is reduced to 62% compared to the controls (photo-irradiated samples without C₆₀@lysozyme and no photo-irradiated cells respectively). Since the photodynamic activity of C₆₀@lysozyme is dose-dependent, the relative medium inhibitory concentrations (IC₅₀) was estimated. The value of the IC₅₀ upon 1 h of low-energy power light irradiation is 3.32 \pm 0.36 μ M.

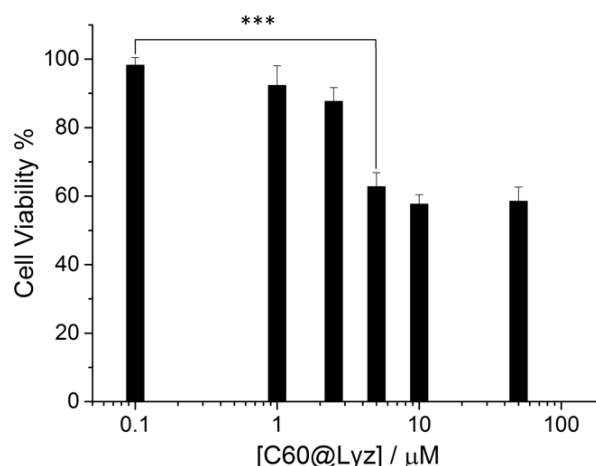


Figure 5. Cytotoxicity study of different concentrations of C₆₀@lysozyme [C60@Lyz]. Samples exposed for 1h to a low-energy power light irradiation (0.064 mWcm⁻²) and incubated 24h before counting. Each value represents the mean value \pm standard deviation (SD) of three experiments and the cell viability is normalized by the control treated in strictly dark condition.

Since in PBS buffer a stronger irradiation produced more ROS than a milder one, we repeated the same experiment with a more intense light source. Using the strong light source, no reduction in the cell viability was observed only for the first 10 min of irradiation, then increasing the irradiation time (Figure S2) the cell viability significantly decreases. Because of the strong effect after 10 minutes, the experiments were carried out only for 5 and 10 min, to avoid the intrinsic photo-toxicity of the lamp.

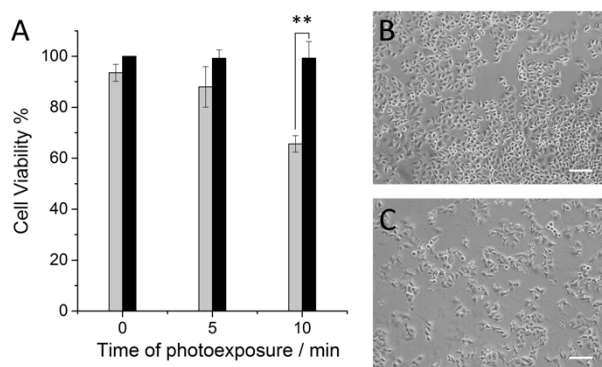


Figure 6. (A) Effect on cell viability upon photo-irradiation with high-power energy source (1.6 mWcm^{-2}) as a function of time. Samples are in the absence (black bars) or in the presence (grey bars) of $5 \mu\text{M}$ of $\text{C}_{60}\text{@lysozyme}$. Each value represents the mean value \pm standard deviation (SD) of three experiments. Phase contrast images of HeLa cells in the absence (B) and in presence (C) of $5 \mu\text{M}$ of $\text{C}_{60}\text{@lysozyme}$ after 10 min of irradiation. (Scale bar: $100 \mu\text{m}$).

Ten minutes of irradiation with the more intense light should generate the same quantity of ROS generated upon 60 min of irradiation with the milder light as showed in the previous paragraph, and in fact the effect on the cells is very similar (Figure 6) and after 10 minutes of irradiation the cell viability decreases to 60%.

Generation of Intracellular ROS

The generation of H_2O_2 due to the photoactivity of $\text{C}_{60}\text{@lysozyme}$ causes oxidative stress and cell death since hydrogen peroxide easily permeates through the membranes and activates endogenous ROS production.

The generation of ROS in the PBS buffer was previously evidenced from the fluorescence enhancement of DCF upon photoexposure of the $\text{C}_{60}\text{@lysozyme}$ solution. Also the measurement of the intracellular ROS is based on the DCFH-DA molecule, that is able to permeate the cell membrane, and is hydrolyzed by the cellular esterases to DCFH, and in the presence of intracellular ROS is oxidized to the highly fluorescent DCF.⁸¹ The fluorescent intensity of DCF in the cell is an indirect measure of intracellular ROS levels, and gives useful information about the toxic effects of $\text{C}_{60}\text{@lysozyme}$ on living cells. The cells treated with $\text{C}_{60}\text{@lysozyme}$ and irradiated (Figure 7C-c) showed a considerable increase in levels of DCF fluorescence, while the cells with the same concentration of $\text{C}_{60}\text{@lysozyme}$, kept in the dark (Figure 7D-d), or cells without $\text{C}_{60}\text{@lysozyme}$, irradiated (Figure 7F-f) or kept in the dark, (Figure 7G-g) does not show a significant fluorescence signal. As a positive control, and for comparison, the HeLa cells were exposed to $200 \mu\text{M}$ H_2O_2 , and as a result they also showed significant fluorescence signal (Figure 7E-e). It is well-known that treatment of HeLa cells with hydrogen peroxide causes intracellular accumulation of ROS,⁸⁶ and the effects are similar to that described for the $\text{C}_{60}\text{@lysozyme}$ upon irradiation. In order to discriminate the amount of oxidative stress induced by the $\text{C}_{60}\text{@lysozyme}$ or by irradiation system, we measured quantitatively the fluorescence intensities.

The increase in DCF fluorescence after illumination is shown in Figure 10A. Fluorescence intensity displays a 4-fold increases in DCF fluorescence for the cells treated with $\text{C}_{60}\text{@lysozyme}$, as compared to the light-treated controls, showing a clear effect of the ROS generation by $\text{C}_{60}\text{@lysozyme}$. The fluorescence signal is mainly located in the perinuclear region (Figure 10H-h).

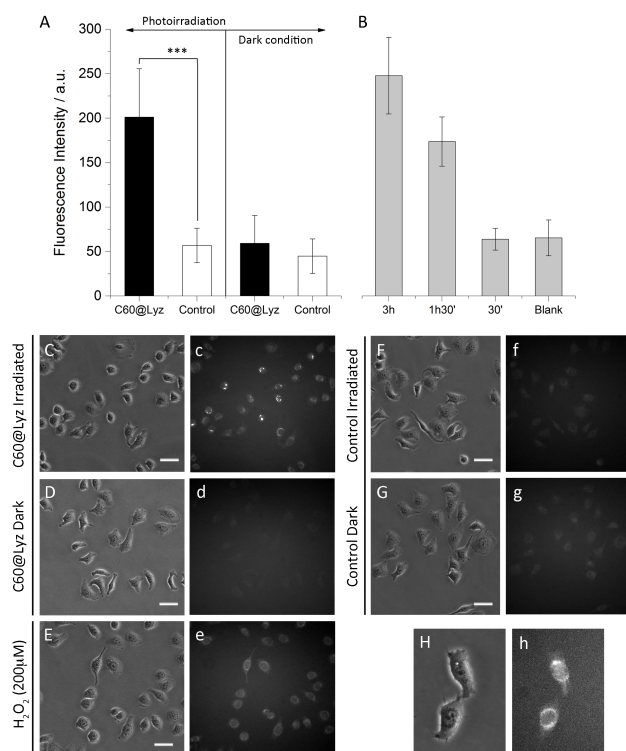


Figure 7. (A) DCF fluorescence intensity (a.u.) upon 10 min photo-irradiation with high-power energy source (1.6 mWcm^{-2}). Samples are in the absence (white bars) or in the presence (black bars) of $5 \mu\text{M}$ of $\text{C}_{60}\text{@lysozyme}$, [$\text{C}_{60}\text{@Lyz}$]. Each value represents the mean value \pm standard deviation (SD) of three experiments. HeLa cells show an increase in ROS levels upon treatment with $5 \mu\text{M}$ of $\text{C}_{60}\text{@lysozyme}$ upon 10 min of irradiation (C-c) as compared to the cells kept under dark conditions (D-d), the photo-irradiated control cells without $\text{C}_{60}\text{@lysozyme}$ (F-f) and the untreated cells (G-g). Treated cells with $200 \mu\text{M}$ of H_2O_2 for 3h were used as positive control (E-e). (B) DCF fluorescence intensity (a.u.) upon different exposition time of the HeLa cells to the solution $200 \mu\text{M}$ of H_2O_2 . (H-h) Enlargement of the cells in the panels C-c. Panels (c-h) were acquired using fluorescence microscopy with 485/20 nm excitation and 535/40 nm emission filter sets after incubating cells with $100 \mu\text{M}$ of DCFH-DA for 30 min following appropriate treatment, while panels (C-H) show the bright field images (transmission).

Conclusions

$\text{C}_{60}\text{@lysozyme}$ hybrid is able to produce singlet oxygen in water upon visible light irradiation as proved by the near IR

emission of $^1\text{O}_2$ around 1270 nm. The ROS generation ability of C₆₀@lysozyme in PBS buffer was demonstrated quantitatively by DCF test. The photoactivity of C₆₀@lysozyme depends on intensity of the radiation, concentration of C₆₀@lysozyme and irradiation time. In the dark C₆₀@lysozyme does not produce ROS, confirming that the photoactivity of C₆₀@lysozyme occurs only upon visible light irradiation.

C₆₀@lysozyme significantly reduced HeLa cells viability in response to visible light and after only 10 minutes of irradiation the cell viability is decreased to 60%.

Intracellular ROS were detected after visible light exposure of C₆₀@lysozyme showing that the hydrogen peroxide produced upon irradiation easily permeates through the membranes and activates endogenous ROS production.

These results indicate that C₆₀@lysozyme is phototoxic and is a promising photosensitizer for PDT. The protein platform could also be improved since it offers different chemical groups for functionalization with:

- i) tumor-targeting tags to improve the cancer cell selectivity and promote the cellular uptake of the photosensitizing agent;
- ii) imaging tags to create a theranostic platform;
- iii) light-harvesting antennae to enhance the ROS production and to extend the absorption spectrum further into the red.

Acknowledgements

This study was supported by the Italian Ministry of Education, University and Research (MIUR) SIR Programme no. RBSI149ZN9-BIOTAXI funded to MC.

Notes and references

- D. E. J. G. J. Dolmans, D. Fukumura and R. K. Jain, *Nat. Rev. Cancer*, 2003, **3**, 380-387.
- Y. Yamakoshi, S. Sueyoshi, K. Fukuhara, N. Miyata, T. Masumizu and M. Kohno, *J. Am. Chem. Soc.*, 1998, **120**, 12363-12364.
- D. M. Guldi and M. Prato, *Acc. Chem. Res.*, 2000, **33**, 695-703.
- R. Koeppe and N. S. Sariciftci, *Photochem. Photobiol. Sci.*, 2006, **5**, 1122-1131.
- Z. Markovic and V. Trajkovic, *Biomaterials*, 2008, **29**, 3561-3573.
- Z. Chen, L. Ma, Y. Liu and C. Chen, *Theranostics*, 2012, **2**, 238-250.
- X. Zhu, M. Sollogoub and Y. Zhang, *Eur. J. Med. Chem.*, 2016, **115**, 438-452.
- T. Da Ros and M. Prato, *Chem. Commun.*, 1999, 663-669.
- S. K. Sharma, L. Y. Chiang and M. R. Hamblin, *Nanomedicine-UK*, 2011, **6**, 1813-1825.
- P. Mroz, G. P. Tegos, H. Gali, T. Wharton, T. Sarna and M. R. Hamblin, *Photochem. Photobiol. Sci.*, 2007, **6**, 1139-1149.
- A. Trpkovic, B. Todorovic-Markovic and V. Trajkovic, *Arch. Toxicol.*, 2012, **86**, 1809-1827.
- E. M. Hotze, J. Labille, P. Alvarez and M. R. Wiesner, *Environ. Sci. Technol.*, 2008, **42**, 4175-4180.
- A. P. Burlaka, Y. P. Sidorik, S. V. Prylutska, O. P. Matyshevska, O. A. Colub, Y. I. Prylutsky and P. Scharff, *Exp. Oncol.*, 2004, **26**, 326-327.
- B. Zhao, Y.-Y. He, C. F. Chignell, J.-J. Yin, U. Andley and J. E. Roberts, *Chem. Res. Toxicol.*, 2009, **22**, 660-667.
- Y. Iwamoto and Y. Yamakoshi, *Chem. Commun.*, 2006, 4805-807.
- M. Guan, T. Qin, J. Ge, M. Zhen, W. Xu, D. Chen, S. Li, C. Wang, H. Su and C. Shu, *J. Mater. Chem. B*, 2015, **3**, 776-783.
- S. D. Snow, K. E. Park and J.-H. Kim, *Environ. Sci. Technol. Lett.*, 2014, **1**, 290-294.
- Y. Mikata, S. Takagi, M. Tanahashi, S. Ishii, M. Obata, Y. Miyamoto, K. Wakita, T. Nishisaka, T. Hirano, T. Ito, M. Hoshino, C. Ohtsuki, M. Tanihara and S. Yano, *Bioorg. Med. Chem. Lett.*, 2003, **13**, 3289-3292.
- E. Otake, S. Sakuma, K. Torii, A. Maeda, H. Ohi, S. Yano and A. Morita, *Photochem. Photobiol.*, 2010, **86**, 1356-1363.
- S. Yano, M. Naemura, A. Toshimitsu, M. Akiyama, A. Ikeda, J.-Kikuchi, X. Shen, Q. Duan, A. Narumi, M. Inoue, K. Ohkubo and S. Fukuzumi, *Chem. Commun.*, 2015, **51**, 16605-16608.
- Q. Liu, L. Xu, X. Zhang, N. Li, J. Zheng, M. Guan, X. Fang, C. Wang and C. Shu, *Chem. Asian J.*, 2013, **8**, 2370-2376.
- D. Franskevych, K. Palyvoda, D. Petukhov, S. Prylutska, I. Grynuk, C. Schuetze, L. Drobot, O. Matyshevska and U. Ritter, *Nanoscale Res. Lett.*, 2017, **12**, 40.
- F. Rancan, M. Helmreich, A. Mölich, N. Jux, A. Hirsch, B. Röder, C. Witt and F. Böhm, *J. Photoch. Photobiol. B*, 2005, **80**, 1-7.
- Y.-Y. Huang, S. K. Sharma, R. Yin, T. Agrawal, L. Y. Chiang and M. R. Hamblin, *J. Biomed. Nanotechnol.*, 2014, **10**, 1918-1936.
- P. Mroz, A. Pawlak, M. Satti, H. Lee, T. Wharton, H. Gali, T. Sarna and M. R. Hamblin, *Free Radical Bio. Med.*, 2007, **43**, 711-719.
- D. S. Kwag, K. Park, K. T. Oh and E. S. Lee, *Chem. Commun.*, 2013, **49**, 282-284.
- P. Mroz, Y. Xia, D. Asanuma, A. Konopko, T. Zhiyentayev, Y.-Y. Huang, S. K. Sharma, T. Dai, U. J. Khan, T. Wharton and M. R. Hamblin, *Nanomed-Nanotechnol.*, 2011, **7**, 965-974.
- X. Qiao, C. Huang, Y. Ying, X. Yang, Y. Liu and Q. Tian, *J. Photoch. Photobiol. B*, 2010, **98**, 193-198.
- K. Irie, Y. Nakamura, H. Ohigashi, H. Tokuyama, S. Yamago and E. Nakamura, *Biosci. Biotech. Biochem.*, 1996, **60**, 1359-1361.
- M. G. Alvarez, C. Prucca, M. E. Milanesio, E. N. Durantini and V. Rivaola, *Int. J. Biochem. Cell. B.*, 2006, **38**, 2092-2101.
- C. Yu, T. Canteenwala, L. Y. Chiang, B. Wilson and K. Pritzker, *Synthetic Met.*, 2005, **153**, 37-40.
- Y. Tabata, Y. Murakami and Y. Ikada, *Jpn. J. Cancer Res.*, 1997, **88**, 1108-1116.
- D. S. Kwag, N. M. Oh, Y. T. Oh, K. T. Oh, Y. S. Youn and E. S. Lee, *Int. J. Pharmaceut.*, 2012, **431**, 204-209.
- Z. Lu, T. Dai, L. Huang, D. B. Kurup, G. P. Tegos, A. Jahnke, T. Wharton and M. R. Hamblin, *Nanomedicine-UK*, 2010, **5**, 1525-1533.
- F. F. Sperandio, S. K. Sharma, M. Wang, S. Jeon, Y.-Y. Huang, T. Dai, S. Nayka, S. C.O.M. de Sousa, L. Y. Chiang and M. R. Hamblin, *Nanomed-Nanotechnol.*, 2013, **9**, 570-579.
- A. S. Stasheuski, V. A. Stupak, B. M. Dzhagarov, M. J. Choi, B. H. Chung and J. Y. Jeong, *Photochem. Photobiol.*, 2014, **90**, 997-1003.
- A. R. Wielgus, B. Zhao, C. F. Chignell, D.-N. Hu and J. E. Roberts, *Toxicol. Appl. Pharm.*, 2010, **242**, 79-90.
- J. Liu, S. Ohta, A. Sonoda, M. Yamada, M. Yamamoto, N. Nitta, K. Murata and Y. Tabata, *J. Control Release*, 2007, **117**, 104-110.
- F. Rancan, M. Helmreich, A. Mölich, E. A. Ermilov, N. Jux, B. Röder, A. Hirsch and F. Böhm, *Bioconjugate Chem.*, 2007, **18**, 1078-1086.

- 40 M. Wang, L. Huang, S. K. Sharma, S. Jeon, S. Thota, F. F. Sperandio, S. Nayka, J. Chang, M. R. Hamblin and L. Y. Chiang, *J. Med. Chem.*, 2012, **55**, 4274-4285.
- 41 M. Wang, S. Maragani, L. Huang, S. Jeon, T. Canteenwala, M. R. Hamblin and L. Y. Chiang, *Eur. J. Med. Chem.*, 2013, **63**, 170-184.
- 42 L. Huang, Y. Xuan, Y. Koide, T. Zhiyentayev, M. Tanaka and M. R. Hamblin, *Laser. Surg. Med.*, 2012, **44**, 490-499.
- 43 Z. Hu, C. Zhang, Y. Huang, S. Sun, W. Guan and Y. Yao, *Chem-Biol. Interact.*, 2012, **195**, 86-94.
- 44 J. Fan, G. Fang, F. Zeng, X. Wang and S. Z. Wu, *Small*, 2013, **9**, 613-621.
- 45 S. Thota, M. Wang, S. Jeon, S. Maragani, M. R. Hamblin and L. Y. Chiang, *Molecules*, 2012, **17**, 5225-5243.
- 46 A. Ikeda, T. Iizuka, N. Maekubo, R. Aono, J. Kikuchi, M. Akiyama, T. Konishi, T. Ogawa, Norihiro, I. Kitagawa, H. Tatebe and K. Shiozaki, *ACS Med. Chem. Lett.*, 2013, **4**, 752-756.
- 47 D. Iohara, M. Hiratsuka, F. Hirayama, K. Takeshita, K. Motoyama, H. Arima and K. Uekama, *J. Pharm. Sci.*, 2012, **101**, 3390-3397.
- 48 K. Nobusawa, M. Akiyama, A. Ikeda and M. Naito, *J. Mater. Chem.*, 2012, **22**, 22610-22613.
- 49 K. Shen, M. A. Gondal, R. G. Siddique, S. Shi, S. Wang, J. Sun and Q. Xu, *Chin. J. Chem.*, 2014, **32**, 78-84.
- 50 W. Zhang, X. Gong, C. Liu, Y. Piao, Y. Sun and G. Diao, *J. Mater. Chem. B*, 2014, **2**, 5107-5115.
- 51 R. A. N. Pertile, F. K. Andrade, C. Alves Jr. and M. Gama, *Carbohydr. Polym.*, 2014, **101**, 692-698.
- 52 L. Feng, S. Yasukazu and M. Nobuhiko, *Oncol. Res.*, 2011, **19**, 203-216.
- 53 T. Metanawin, T. Tang, R. Chen, D. Vernon and X. Wang, *Nanotechnology*, 2011, **22**, 235604-13.
- 54 A. Ikeda, M. Matsumoto, M. Akiyama, J. Kikuchi, T. Ogawa and T. Takeya, *Chem. Commun.*, 2009, **12**, 1547-1549.
- 55 A. Ikeda, Y. Doi, K. Nishiguchi, K. Kitamura, M. Hashizume, J. Kikuchi, K. Yogo, T. Ogawa and T. Takeya, *Org. Biomol. Chem.*, 2007, **5**, 1158-1160.
- 56 Y. Doi, A. Ikeda, M. Akiyama, M. Nagano, T. Shigematsu, T. Ogawa, T. Takeya and T. Nagasaki, *Chem. Eur. J.*, 2008, **14**, 8892-8897.
- 57 A. Ikeda, M. Nagano, M. Akiyama, M. Matsumoto, S. Ito, M. Mukai, M. Hashizume, J. Kikuchi, K. Katagiri, T. Ogawa and T. Takeya, *Chem. Asian J.*, 2009, **4**, 199-205.
- 58 A. Ikeda, M. Akiyama, T. Ogawa and T. Takeya, *ACS Med. Chem. Lett.*, 2010, **1**, 115-119.
- 59 A. Ikeda, T. Sue, M. Akiyama, K. Fujioka, T. Shigematsu, Y. Doi, J. Kikuchi, T. Konishi, and R. Nakajima, *Org. Lett.*, 2008, **10**, 4077-4080.
- 60 S.-I. Yusa, S. Awa, M. Ito, T. Kawase, T. Takada, K. Nakashima, D. Liu, S. Yamago and Y. Morishima, *J. Polym. Sci. Pol. Chem.*, 2011, **49**, 2761-2770.
- 61 M. Akiyama, A. Ikeda, T. Shintani, Y. Doi, J. Kikuchi, T. Ogawa, K. Yogo, T. Takeya and N. Yamamoto, *Org. Biomol. Chem.*, 2008, **6**, 1015-1019.
- 62 M. O. Davydenko, E. O. Radchenko, V. M. Yashchuk, I. M. Dmitruk, Y. I. Prylutsky, O. P. Matishevska and A. A. Golub, *J. Mol. Liq.*, 2006, **127**, 145-147.
- 63 X. Qu, T. Komatsu, T. Sato, O. Glatter, H. Horinouchi, K. Kobayashi and E. Tsuchida, *Bioconjugate Chem.*, 2008, **19**, 1556-1560.
- 64 T. Komatsu, A. Nakagawa and X. Qu, *Drug Metab. Pharmacok.*, 2009, **24**, 287-299.
- 65 S.-R. Chae, A. R., Badireddy, J. F. Budarz, S. Lin, Y. Xiao, M. Therezien and M. R. Wiesner, *ACS Nano*, 2010, **4**, 5011-5018.
- 66 S. Deguchi, S. Mukai, M. Tsudome and K. Horikoshi, *Adv. Mater.*, 2006, **18**, 729-732.
- 67 G. V. Andrievsky, M. V. Kosevich, O. M. Vovk, V. S. Shelkovsky and L. A. Vashchenko, *J. Chem. Soc., Chem. Commun.*, 1995, 1281-1282.
- 68 S. Deguchi, R. G. Alargova and K. Tsujii, *Langmuir*, 2001, **17**, 6013-6017.
- 69 A. Hirsch, *Angew. Chem. Int. Ed. Engl.*, 1993, **32**, 1138-1141.
- 70 E. Nakamura and H. Isobe, *Acc. Chem. Res.*, 2003, **36**, 807-815.
- 71 M. Dallavalle, M. Leonzio, M. Calvaresi and F. Zerbetto, *ChemPhysChem*, 2014, **15**, 2998-3005.
- 72 D. Canevet, E. M. Pérez and N. Martín, *Angew. Chem. Int. Ed.*, 2011, **50**, 9248-9259.
- 73 S. Samal and K. E. Geckeler, *Chem. Commun.*, 2001, 2224-2225.
- 74 V. J. Stella and Q. He, *Toxicol. Pathol.*, 2008, **36**, 30-42.
- 75 M. Calvaresi, F. Arnesano, S. Bonacci, A. Bottoni, V. Calò, S. Conte, G. Falini, S. Fermani, M. Losacco, M. Montalti, G. Natile, L. Prodi, F. Sparla and F. Zerbetto, *ACS Nano*, 2014, **8**, 1871-1877.
- 76 M. Calvaresi, A. Bottoni and F. Zerbetto, *J. Phys. Chem. C*, 2015, **119**, 28077-28082.
- 77 M. Calvaresi and F. Zerbetto, *Acc. Chem. Res.*, 2013, **46**, 2454-2463.
- 78 M. Calvaresi, S. Furini, C. Domene, A. Bottoni and F. Zerbetto, *ACS Nano*, 2015, **9**, 4827-4834.
- 79 M. Calvaresi and F. Zerbetto, *Nanoscale*, 2011, **3**, 2873-2881.
- 80 F. Trozzi, T. D. Marforio, A. Bottoni, F. Zerbetto and M. Calvaresi, *Isr. J. Chem.*, 2016, DOI: 10.1002/ijch.201600127.
- 81 C. P. LeBel, H. Ischropoulos and S. C. Bondy, *Chem. Res. Toxicol.*, 1992, **5**, 227-231.
- 82 J. Zhao and M. Riediker, *J. Nanopart. Res.*, 2014, **16**, 2493.
- 83 S. Saha, R. Majumdar, M. Roy, R. R. Dighe and A. R. Chakravarty, *Inorg. Chem.*, 2009, **48**, 2652-2663.
- 84 P. Riesz, D. Berdahl and C. L. Christman, *Environ. Health Perspect.*, 1985, **64**, 233-252.
- 85 J. Lee, J. D. Fortner, J. B. Hughes and J. H. Kim, *Environ. Sci. Technol.* 2007, **41**, 2529-2535.
- 86 B. V. Chernyak, D. S. Izyumov, K. G. Lyamzaev, A. A. Pashkovskaya, O. Y. Pletjushkina, Y. N. Antonenko, D. V. Sakharov, K. W. A. Wirtz and V. P. Skulachev, *Biochim. Biophys. Acta* 2006, **1757**, 525-534.